Journal of the European Ceramic Society **18** (1998) 1201–1210
© 1998 Elsevier Science Limited
Printed in Great Britain. All rights reserved
PII: S0955-2219(98)00043-0
0955-2219/98/$—see front matter

Structural and Textural Study on ZrO_2–Y_2O_3 Powders

M. R. Álvarez,[a]* A. R. Landa,[b] L. C. Otero-Díaz[a] and M. J. Torralvo[a]†

[a]Departamento Química Inorgánica I. Universidad Complutense de Madrid, E-28040 Madrid, Spain
[b]Centro de Microscopía Electrónica. Universidad Complutense de Madrid, E-28040 Madrid, Spain

Abstract

Microporous gels of ZrO_2, ZrO_2·2mol% Y_2O_3 and ZrO_2·5mol% Y_2O_3 were treated in air and under vacuum at temperatures ranging from 450 to 1300°C. X-ray and electron diffraction results seem to indicate that both, pure and doped zirconia gels crystallize in the cubic form of ZrO_2. On lengthening of the thermal treatment at 450°C or after treatment at higher temperatures, the transformations cubic→tetragonal→monoclinic occur, but those are delayed as the yttria content in the sample increases. In some treatment conditions, cubic and tetragonal phases can also been retained to some extent in pure zirconia. Moreover, a rhombohedral deformation of the cubic cell along the ⟨111⟩ directions has been observed in some crystals of pure zirconia samples. Textural degradation takes place in both, pure and doped zirconia, due to particle growth and also the loss of porosity and therefore, the observed structural stabilization does not improve textural stability. The differences in the texture of pure and doped samples have been related to dehydration and crystal growth processes, and to the properties of primary particles in the gels. © *1998 Elsevier Science Limited. All rights reserved*

1 Introduction

Fundamental researchs and studies about the properties and processing of zirconia based materials are widely reported in the literature.[1,2] The utility of these solids as ceramic precursors, catalysts or solid electrolytes, and the possibility that microstructure of materials can be designed and optimized, justify the interest that zirconia and doped zirconia arouse.[3–6]

In doped zirconia, the transformation from the high temperature phases of ZrO_2, cubic (c) and tetragonal (t), to the monoclinic (m) phase are prevented and this fact allows to take advantage of these materials. With the addition of dopant, the chemical free energy of each polymorph changes in such a way, that the cubic and/or tetragonal phases can be stabilized at room temperature. Moreover, a surface energy effect also contributes to the stability of the phases in pure and doped zirconia, because superficial energy corresponding to the monoclinic phase is higher than that of tetragonal phase. In yttria-doped zirconia, since the mass transport by surface diffusion is lower than for zirconia, crystal growth is hindered and phase transitions are delayed.[7–12]

On the other hand, the texture of powdered zirconia degrades during thermal treatment and therefore, the use of zirconia as catalyst or as pigment requires the improvement of textural stability. Since the loss of surface area occurs to some extent by the growth of the particles, and this process also affects to phase transformations, textural degradation and structural changes have been related.[11] Researchs have been done related to this, and it has been reported that mesoporous yttria-doped zirconia with more stable texture was prepared.[11,13]

This work is concerned with fundamental studies about textural and structural changes in pure and doped zirconia. Samples obtained from microporous gels and treated in several conditions, have been characterized by X-ray and electron diffraction, electron microscopy and gas adsorption measurements. In order to study the structural evolution during thermal treatment, in situ high temperature X-ray experiments have been carried out.

†To whom correspondence should be addressed.

Present address: Dpto. Q. Inorgánica y Materiales, Universidad San Pablo CEU, E-28668 Boadilla del Monte (Madrid), Spain.

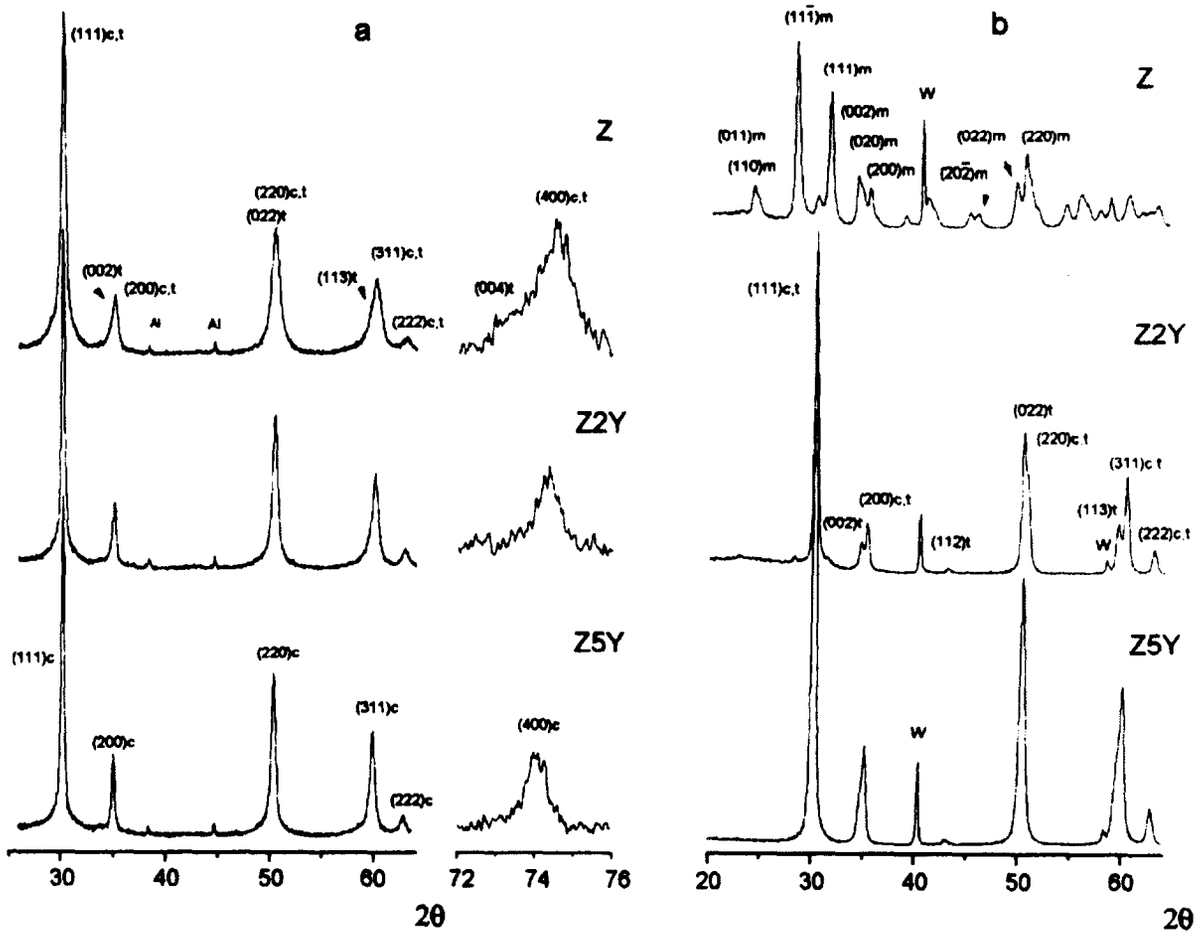

Fig. 1. X-ray diffraction patterns of the samples obtained from Z, Z2Y and Z5Y gels by heating in air at (a) 450°C for 2 h, and (b) 800°C for 30 days.

2 Materials and Methods

The samples were prepared from ZrO_2, ZrO_2·2mol%Y_2O_3 and ZrO_2·5mol%Y_2O_3 microporous gels, by heating in air and under vacuum. The starting gels were obtained from $ZrOCl_2 \cdot 8H_2O$ and $YCl_3 \cdot 6H_2O$ solutions in water, by hydrolysis with ammonia up to a value of final pH of 10·5. The products were filtered, washed with water and dried over $CaCl_2$.[14,15] The gels are denoted Z, Z2Y and Z5Y, respectively. Treatments in air were carried out at 110°C for 6 h and from 450 to 1300°C for variable times from 2 h to 30 days. The gels were also treated under vacuum ($\cong 10^{-1}$ Pa) up to 450°C at a heating rate of 2° min^{-1}. These materials were characterized by X-ray and electron diffraction, electron microscopy and nitrogen and argon adsorption at −196°C.

X-ray powder diffraction patterns were recorded with a Siemens D5000 diffractometer using Cu K_α radiation. The diagrams were scanned in steps of 0·02° (2θ) and with a 3 s per step counting time. A Jeol 2000 FX electron microscope operating at 200 kV and fitted with a XEDS detector, AN10000 LINK system, was used in the transmission electron microscopy study.

The adsorption–desorption isotherms of nitrogen and argon were determined using the conventional static procedure. Prior to the adsorption the samples were degassed at 120°C down to about 10^{-1} Pa. The adsorption data were analyzed by the BET equation and the α_s method, using as standard Ar/silica isotherms.[16] Pore size distributions were obtained from the adsorption branch of the isotherms using the Kelvin equation.[17] Cross-sectional areas of 0·138 and 0·162 nm^2 were used for adsorbed molecules of nitrogen and argon, respectively.[18]

The study of the structural evolution in vacuum (residual pressure of 3–5 Pa) was carried out using an Anton Paar HTK10 high-temperature camera coupled to the X-ray diffractometer. Heating–cooling cycles with top temperature of 900, 1000 and 1300°C were made with different portions of the gels placed on the Pt filament. In all cycles, the heating-cooling rate was 1° min^{-1}. Diffraction patterns were collected each 50° in temperature with a dwell time of 30 min at each temperature. Diagrams were recorded from 25 to 55° (2θ) in steps of 0·02° and with 1 s per step counting time. The samples obtained at room temperature after the heating–cooling cycles were also characterized by electron diffraction and electron microscopy.

In some of the included figures, the samples have been labelled as $X(T/t\text{A})$ and $X(T/\text{V})$, where: $X = Z$, Z2Y, Z5Y; T = treatment top temperature;

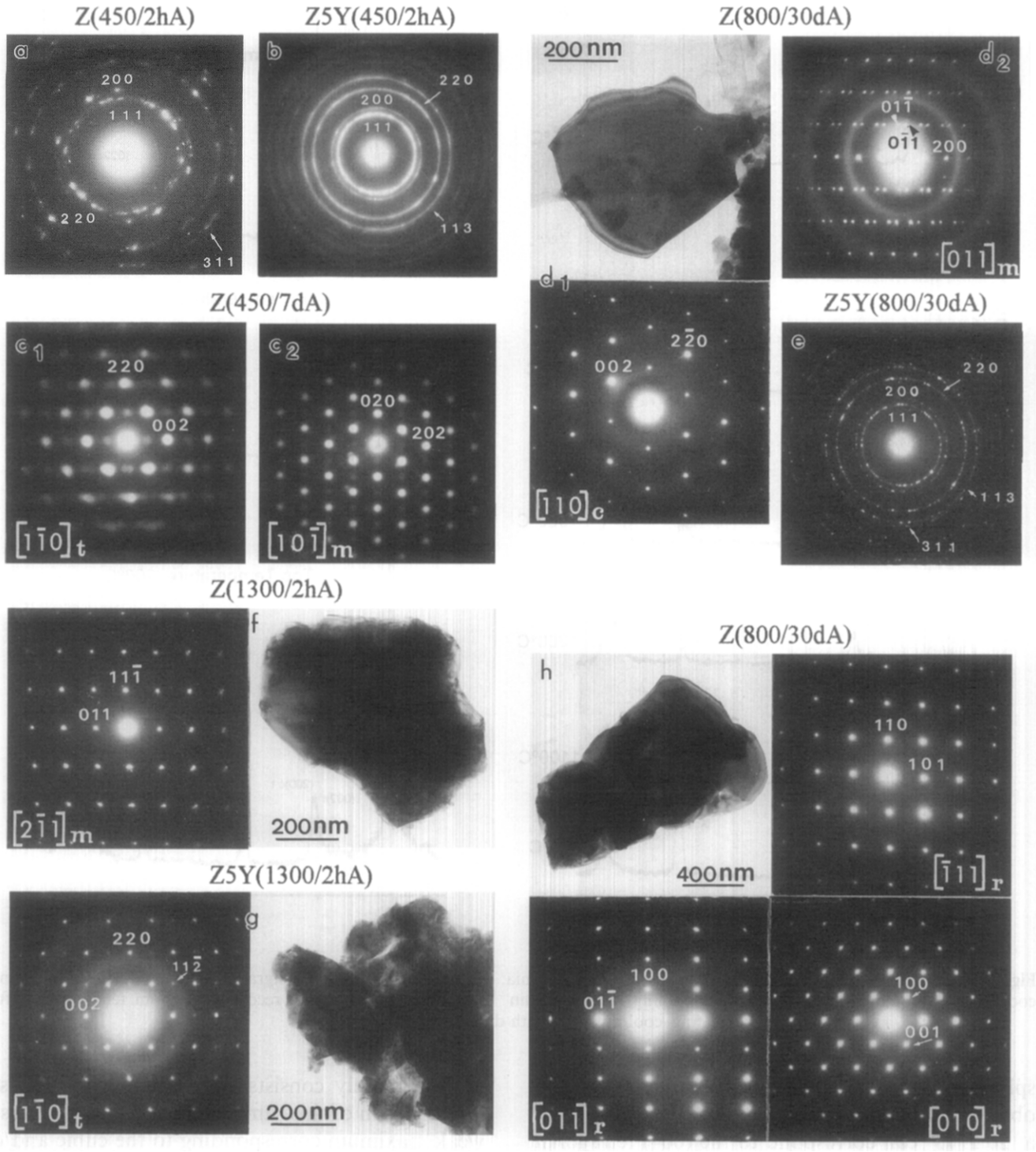

Fig. 2. TEM micrographs and SAED diagrams corresponding to the samples obtained in air after treatment at (a, b) 450°C for 2 h and (c_1, c_2) 7 days; (d_1, d_2, e, h) 800°C during 30 days, and (f, g) 1300°C for 2 h. The micrograph and diagrams in (h) correspond to the same crystal.

t = treatment dwell time (2 h, 20 h, 7 days, 30 days); A = air and V = vacuum.

3 Results

XEDS spectra corresponding to Z gel only show peaks from zirconium and oxygen and for doped gels, peaks from yttrium are also observed. In the three types of samples, the analyzed particles present similar spectra in each case. As expected, the observed intensity ratio of the Zr/Y peaks for Z5Y samples is higher than for the Z2Y ones.

In Fig. 1 are collected the X-ray diffraction patterns of the samples obtained from Z, Z2Y and Z5Y gels by treatment in air at 450°C for 2 h [Fig. 1(a)] and at 800°C for 30 days [Fig. 1(b)]. In Fig. 1(a), the diagrams of doped samples correspond to the cubic form of ZrO_2, but for pure zirconia sample a mixture of cubic and tetragonal phases must be present. In this last case, the (200), (220), (311) and (400) cubic reflections show not

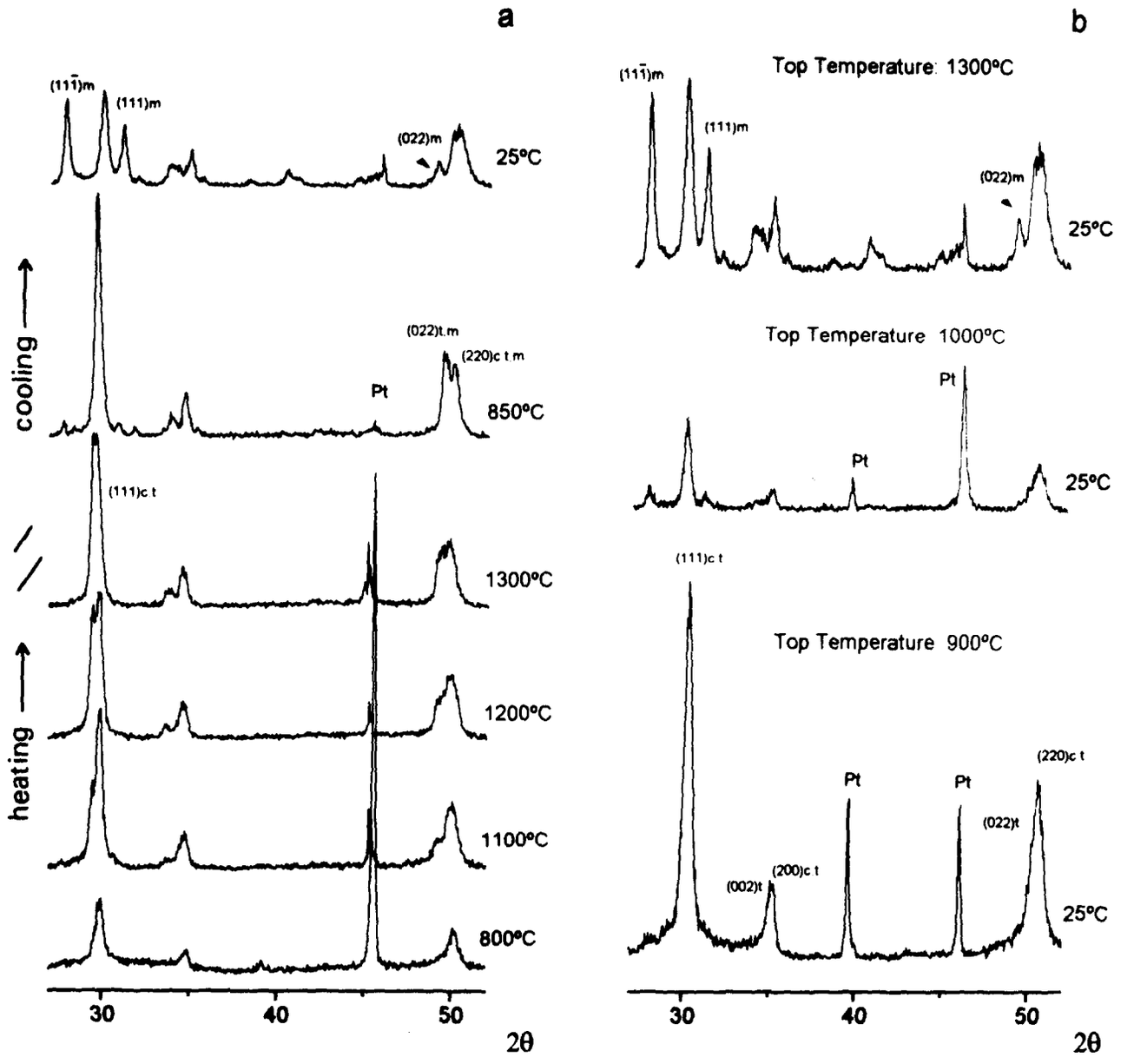

Fig. 3. X-ray diffraction patterns corresponding to pure zirconia: (a) more representative diagrams recorded during the heating-cooling cycle up to 1300°C with heating-cooling rate of 1° min^{-1}; (b) diffraction patterns recorded at room temperature after heating–cooling cycles with different top temperatures.

splitting, but broadening and asymmetry are observed. In addition, a weak peak which appears at $2\theta \cong 73°$ can correspond to the (004) tetragonal reflection. The diagrams of the samples obtained from Z5Y gel show not change after treatment at 450°C for 30 days, but on lengthening the treatment at 800°C asymmetric maxima corresponding to the (200), (220) and (311) cubic reflections are observed [Fig. 1(b)]. For Z2Y doped samples the splitting of the cubic reflections is clearly observed after treatment at 800°C for 30 days [Fig. 1(b)]. In the case of pure zirconia, the splitting of the cubic reflections together with a weak maximum corresponding to the (11$\bar{1}$) monoclinic line are observed in the diagram of the sample treated at 450°C for 20 h. The intensity of the monoclinic reflections increases when increasing time and/or temperature of treatment, and sample treated at 800°C for 30 days mainly consists of the monoclinic phase. The diagram of this sample [Fig. 1(b)] also shows a weak maximum corresponding to the cubic and/or tetragonal forms. After treatment at 1300°C for 2 h, the diffraction pattern of the sample of pure zirconia only shows reflections corresponding to the monoclinic structure. Doped samples treated at 1300°C for 2 h correspond to the phase with tetragonal symmetry, and for Z2Y doped sample, two weak peak corresponding to the (11$\bar{1}$) and (111) monoclinic reflections are also observed.

Representative transmission electron microscopy (TEM) micrographs and selected area electron diffraction (SAED) diagrams of samples treated in air are collected in Fig. 2. Electron diffraction patterns of pure and doped samples treated at 450°C and for doped samples treated at 800°C are characteristic of polycrystalline materials, and they can

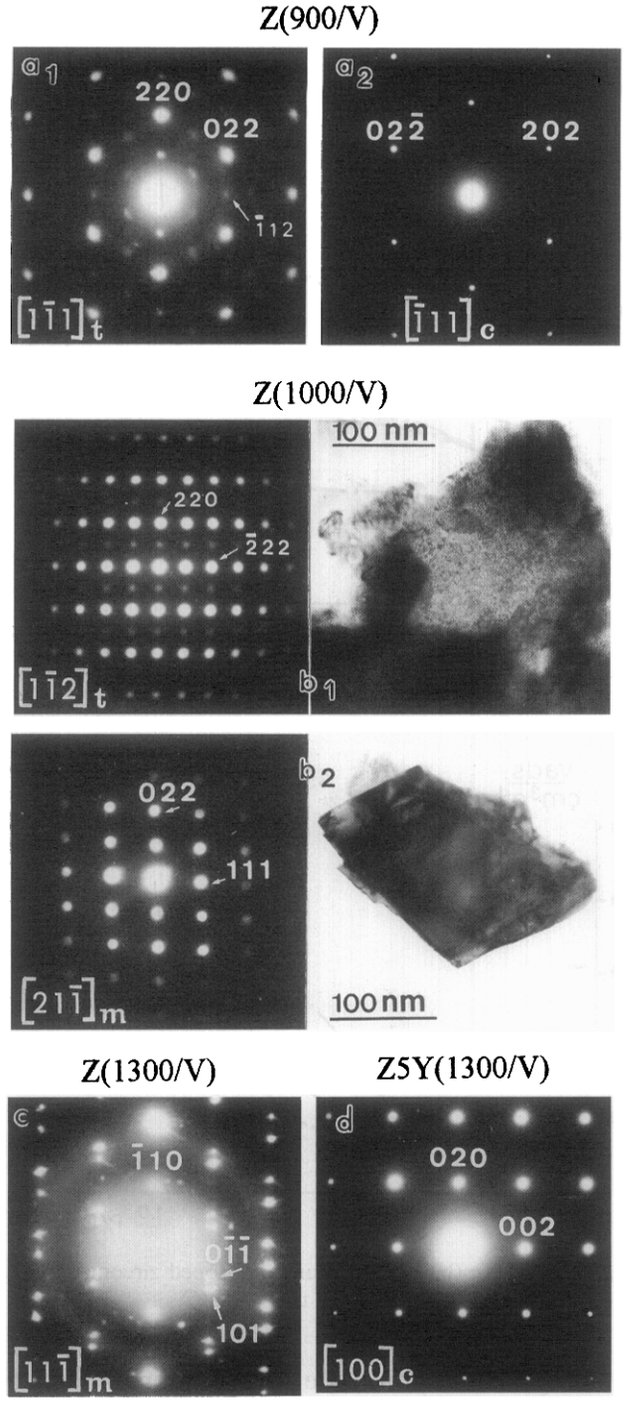

Fig. 4. TEM micrographs and SAED diagrams for the samples obtained at room temperature after the heating-cooling cycles with top temperature of (a_1, a_2) 900°C; (b_1, b_2) 1000°C; (c, d) 1300°C.

correspond to the cubic and/or tetragonal phases [Fig. 2(a)–(c) and (e)]. For pure zirconia samples, microdiffraction patterns have been obtained and they have allowed us to identify in some cases the tetragonal and monoclinic phases [Fig. 2(c_1) and (c_2)]. At temperatures higher than 450°C, pure zirconia samples show diffraction patterns corresponding most of them to a twinned crystal of the monoclinic phase [Fig. 2(d_2) and (f)]. Moreover, some crystals of the sample treated at 800°C for 30 days correspond to the cubic phase [Fig. 2(d_1)]. In this last sample, some crystals show SAED diagrams that could not be indexed on cubic, tetragonal and monoclinic symmetries [Fig. 2(h)]. The indexing of these diagrams has been made in a rhombohedral (r) cell with parameters $a_r \cong 0{\cdot}36$ nm and $\alpha_r = 54{\cdot}5° \pm 0{\cdot}5°$. The observed diffraction patterns for Z5Y doped sample treated at 1300°C for 2 h can be indexed on a tetragonal symmetry cell. In the [1$\bar{1}$0] tetragonal zone axis [Fig. 2(g)] we can observe weak spots corresponding to the (hkl): odd–odd–even reflections which are forbidden for a cubic F cell [Fig. 2(d_1)].

Figure 3(a) shows representative X-ray diffraction patterns corresponding to the pure zirconia gel, recorded in the heating-cooling cycle with top temperature of 1300°C. Diagrams recorded up to 1100°C show diffraction maxima at about $2\theta \cong 30$, 35 and 50°, which could correspond to the cubic form. For the temperatures higher than 1100°C, the splitting of the $2\theta \cong 35$ and 50° maxima occurs and at the same time, a second line at $2\theta \cong 29°$ appears. This second maximum could be assigned to the (111) tetragonal reflection, then, both tetragonal and cubic phases seem to coexist. During cooling down to room temperature, the transformation to the monoclinic phase occurs. Both, the temperature at which the monoclinic lines appear and the proportion of this phase obtained at room temperature are higher when the top temperature increases [Fig. 3(b)]. In Fig. 4 are shown TEM micrographs and SAED diagrams corresponding to the samples obtained at room temperature after the heating-cooling cycles with different top temperatures. In the sample treated up to 900°C both, cubic and tetragonal phases have been identified [Fig. 4(a_1) and (a_2)]. Microdiffraction patterns corresponding to the sample obtained after heating up to 1000°C show the existence of tetragonal phase together with the monoclinic form [Fig. 4(b_1) and (b_2)]. At 1300°C this last polymorph usually appears as twinned crystal [Fig. 4(c)].

In the sample obtained from the Z5Y gel, the X-ray diffraction patterns show not significant changes during heating-cooling cycle up to 1300°C. In Fig. 4(d) is shown the SAED diagram along the [1 0 0] cubic zone axis.

In some crystals of pure zirconia samples obtained after the treatment with top temperatures of 1000 and 1100°C, rhombohedral deformation has also been observed.

Textural study has been carried out in pure and doped zirconia samples treated in air at 450°C for several periods and under vacuum up to 450°C. The samples obtained at higher treatment temperatures present low values of surface area. In Fig. 5 are collected the adsorption–desorption isotherms of nitrogen for Z, Z2Y and Z5Y gels and

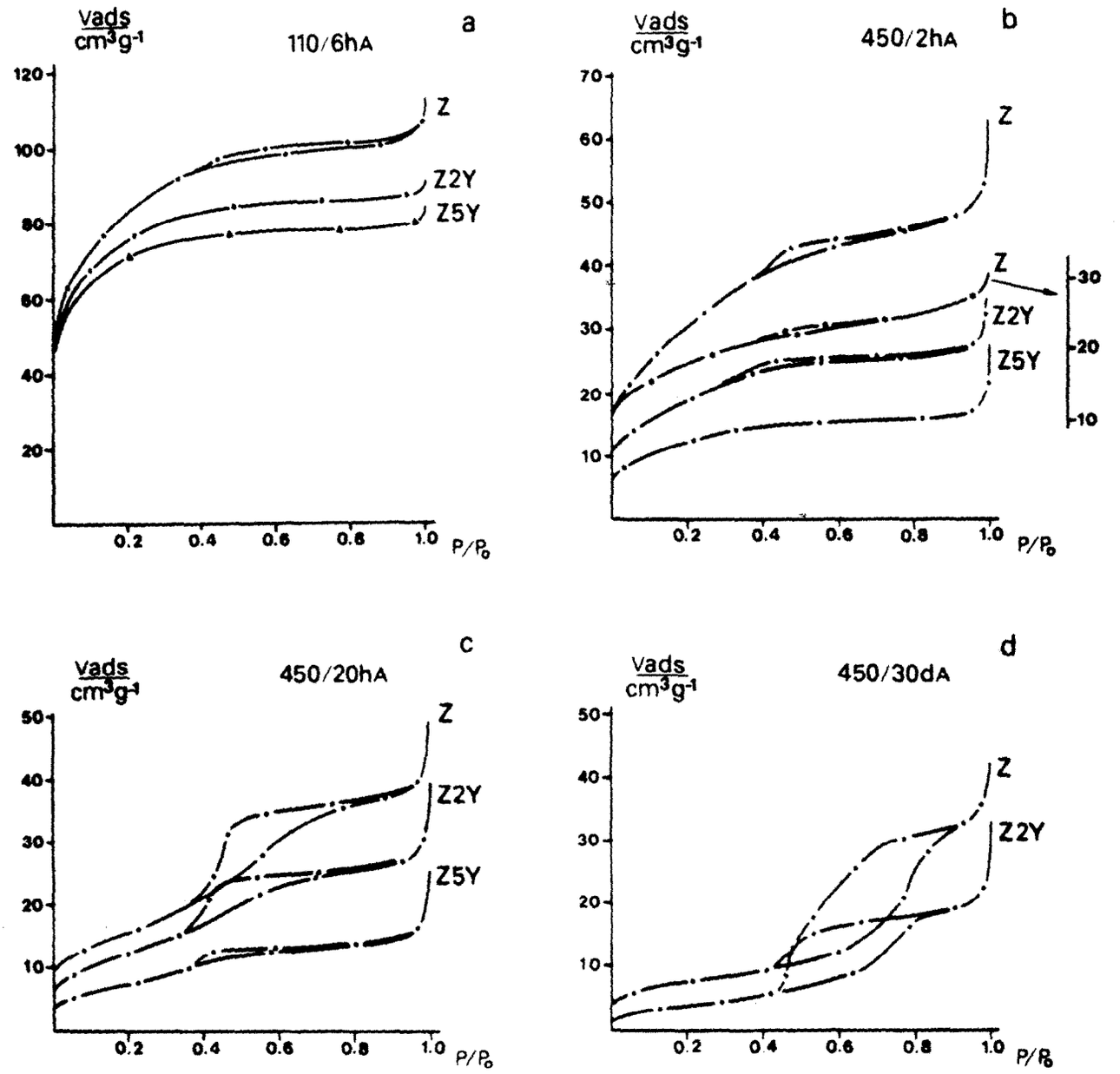

Fig. 5. Adsorption–desorption isotherms of nitrogen for (a) Z, Z2Y and Z5Y gels; (b, c and d) pure and doped zirconia samples treated in air at 450°C for several periods; * pure zirconia treated under vacuum up to 450°C.

the corresponding samples obtained by treatment in air at 450°C for several times. The isotherm of pure zirconia treated under vacuum up to 450°C is also shown in this figure. The pore size distributions corresponding to the samples obtained by heating in air are shown in Fig. 6. In the low pressures region ($P/P_o \sim 0{\cdot}35$, pore radii (r_p)$\sim$1·7 nm) the validity of the Kelvin equation become doubtful.[19] Therefore, pore size distributions in this region are indicated by broken lines.

We can observe that thermal treatment of the microporous gels provokes the decreasing of adsorption capacity in both, pure and doped zirconia. However, for similar treatment conditions, the adsorption capacity decreases with the increase of the yttria content in the sample (Fig. 5). Pure zirconia and 2mol%Y_2O_3-doped samples treated for 30 days are essentially mesoporous with heterogeneous pore size distributions (Fig. 6). Sample obtained by treatment of Z5Y gel in similar conditions shows very low adsorption capacity.

On the other hand, we can also observe in Fig. 5 that pure zirconia treated under vacuum presents adsorption capacity lower than the sample obtained in air and poorly developed mesoporous texture. Doped samples treated in vacuum present surface areas lower than 5 $m^2\ g^{-1}$.

In Fig. 7 are plotted representative α_s-isotherms obtained from argon adsorption at −196°C. In each α_s-plot, the straight line corresponds to monolayer–multilayer adsorption. From the intercept of the extrapolated line to the volume axis, the volume corresponding to narrow micropores have been obtained. These micropores must be lower than about 1 nm in width, according to the molecular size of the adsorbed argon (molecular kinetic

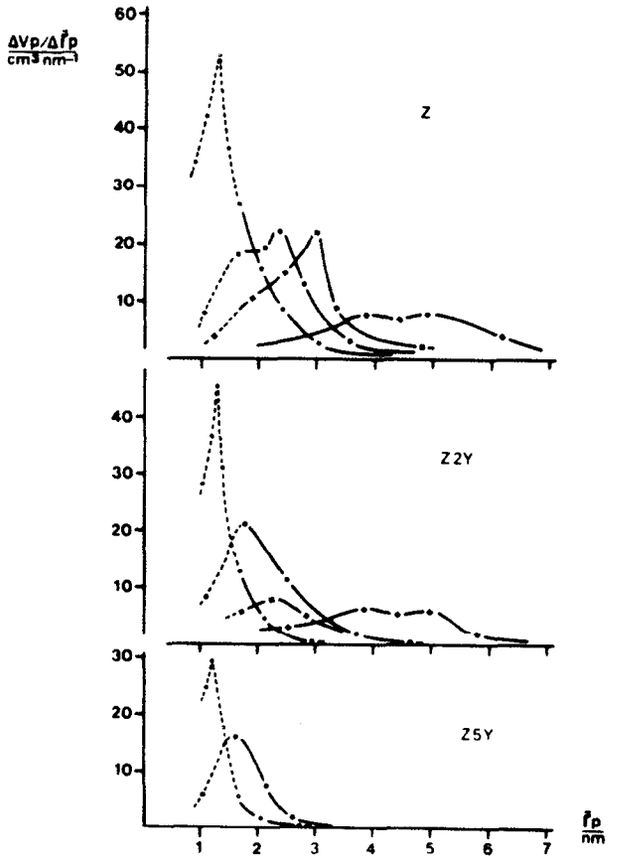

Fig. 6. Pore size distributions obtained from nitrogen adsorption data for Z, Z2Y and Z5Y treated in air at 450°C for (○) 2 h, (●) 20 hm (×) 7 days, (◆) 30 days.

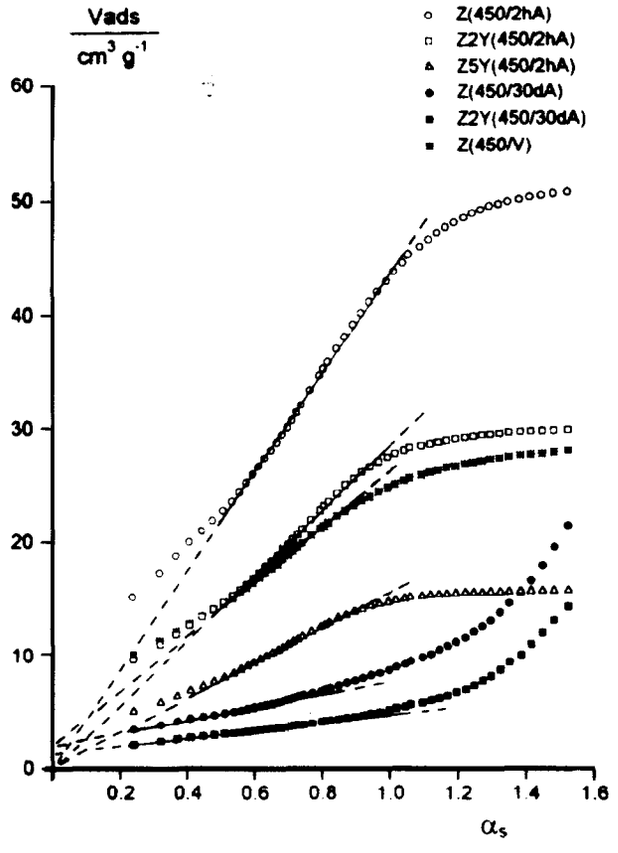

Fig. 7. Representative α_s-plots obtained from argon adsorption data.

diameter for argon: 0·34 nm). From the slope of the straight line, we have calculated the value of surface area ($S\alpha_s$) which correspond to both, the pores larger than about 1 nm in width and the external surface. For the samples treated in different conditions, the variation of BET area (S_{BET}) and cumulative surface area (S_p) in pores with $r_p \sim 1{\cdot}7$ nm, as a function of the yttria content, has been plotted in Fig. 8(a) and (b). From the values of S_{BET}, S_p and $S\alpha_s$ obtained from argon adsorption, we have estimated the contribution of the pores with $r_p \sim 0{\cdot}5$ nm, $0{\cdot}5 \sim r_p \sim 1{\cdot}7$ nm and $r_p \sim 1{\cdot}7$ nm to the total surface area. In Fig. 8(c) are shown the results obtained for pure and doped gels and for the samples treated in air.

4 Discussion

The X-ray and electron diffraction and electron microscopy results can be summarized as follows:

- In both pure and doped zirconia, the cubic phase is present next to crystallization of the amorphous gels. On lengthening of the thermal treatment, transformations to the monoclinic phase (cubic→tetragonal→monoclinic) occur but, they are delayed when increasing the yttria content of the sample.
- In pure zirconia samples, the higher symmetry phases (cubic and tetragonal) are retained to some extent which depends on the treatment conditions. Thus it is higher when heating is carried out under vacuum and when the top temperature and/or treatment time decrease. In doped samples, the tetragonal phase obtained at room temperature must be also a metastable phase according to the phase diagram of ZrO_2–Y_2O_3 system.[20]
- Thermal treatment in air and under vacuum provokes crystal growth but, this effect is more important for undoped zirconia than for doped samples treated under similar conditions.

On the other hand, the textural study results show that:

- During thermal treatment, textural degradation occurs in both pure and doped samples and the loss of adsorption capacity is higher when the treatment is carried out under vacuum.
- For any of the investigated treatment conditions, pure zirconia presents higher values of surface area and pore volume together with more developed mesoporous texture than doped samples.

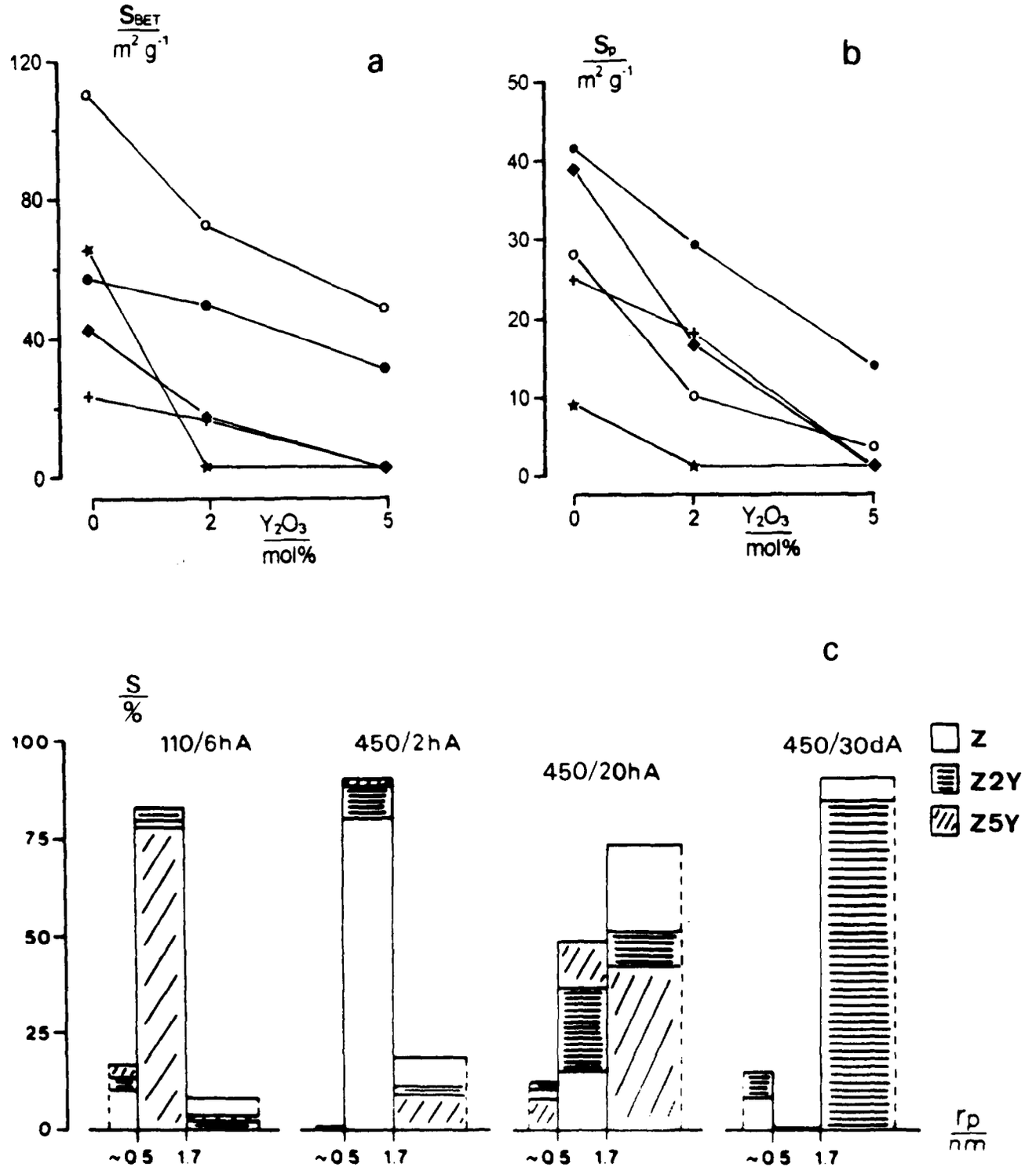

Fig. 8. Variation of (a) BET area and (b) cumulative area, with the yttria content, of samples treated in air at 450°C for (○) 2 h, (●) 20 h, (◆) 7 days and (×) 30 days and * under vacuum up to 450°C; (c) contribution of pores with $r_p \lesssim 0{\cdot}5$ nm, $0{\cdot}5 \lesssim r_p \lesssim 1{\cdot}7$ nm and $r_p \gtrsim 1{\cdot}7$ nm to the total area of Z, Z2Y and Z5Y gels treated in air at 110 and 450°C for several periods.

- The loss of adsorption capacity seems to be due to the elimination of microporosity and to the enlargement of larger pores. The first effect is the most important fact during treatment in vacuum.

Our results concerning the evolution of the textural properties of porous pure zirconia during thermal treatment are in agreement with previous works.[21–24] The loss of surface area is produced by both, the reduction of micropore volume and the widening of larger pores. These facts can be related with dehydration and crystallization processes in the gel[25] together with the growth of the particles. Condensation and elimination of water from inter/intraparticles surface OH^- groups do not need large diffusion path of the atoms and produce the reduction of microporosity at relatively low temperature. Moreover, the reduction of surface area due to the growth of the particles is the main effect taking

place at higher temperatures. Therefore, in doped samples obtained from precursors microporous gels, although crystal growth is inhibited, the collapse of porous structure occurs and the stability of the texture is not improved. On the other hand, for doped samples the loss of porosity is higher than for pure zirconia treated in similar conditions and this fact must be related with the way of packing of the primary particles in the gels. When the precipitation of the gel is carried out at a high pH value, large particles are formed and they are linked together through molecular water hydrogen-bonded to the surface OH^- groups.[26] In the aggregates, the packing of the particles must be affected by the superficial charge and therefore, by the isoelectric point (i.p.) of the sample.[22,27] Although isoelectric points are strongly affected by the preparation conditions, the i.p. of hydrated ZrO_2 must be lower than the corresponding to the doped samples obtained in similar conditions.[28–30] So, the final pH of precipitation of the gels (about 10·5) must be higher than the i.p. of both, pure and doped zirconia samples but closer to the corresponding to doped samples. Therefore, the particles of doped samples which should have a minor superficial charge than that of pure zirconia, could produce weaker and denser aggregates with higher coordination number. In this way, dehydration of doped samples can produce denser aggregates with narrower interparticle pores and this fact must assist the sintering in these materials.

On the other hand, experimental evidences and thermodynamic arguments indicate that the existence of metastable high symmetry phases in both pure and doped zirconia is related with a high value of surface free energy.[7–10] Since particle growth and the elimination of porosity decrease surface energy, both factors must affect to the phase transformations. According to these arguments, ours results about pure zirconia show that loss of porosity and particle growth occur with thermal treatment and, at the same time the transformation to the monoclinic phase is observed. Moreover, in doped samples treated in similar conditions to pure zirconia, the size of the particles is smaller since crystal growth is inhibited. However, doped samples, as pure zirconia, lose surface area due to the elimination of porosity and therefore, surface free energy must decrease during thermal treatment. Addition of Y_2O_3 must produce a change in the chemical free energy of each phase in such a way that phase-transformations are delayed in spite of the surface free energy decreases.

On the other hand, the strains generated by the transformation tetragonal(→monoclinic, could prevent the completion of this transformation and it contributes to retain the high symmetry phases.[9,10,31] The existence of these strains is suggested by the fact that monoclinic phase is twinned and could also justify the rhombohedral deformation observed in some crystals.

Acknowledgements

The authors wish thank to Centro de Microscopía Electrónica (U.C.M.) for facilities. This work was supported by the C.I.C.Y.T research project MAT-95-0809.

References

1. Somiya, S., Yamamoto, N. and Yanagida, H., (eds), Science and Technology of Zirconia 1986. In *Advanced in Ceramics*, Vols. 24A and 24B. The American Ceramic Society, Westerville, OH, 1988.
2. Gasgnier, M., Phase transitions and microstructures of: a) zirconia ceramics as ZrO_2–M_xO_y (M = Y, Sc, Mg, Ca, Al and mullite) systems, b) alumina and $Al_xM_yO_z$ systems. In *Diffussionless Phase Transitions and Related Structures in Oxides*, ed. C. Boulesteix. Key Engineering Materials, Vol. 68. Trans. Tech. Publications, Zurich, Switzerland, 1992, pp. 247–292.
3. Heuer, A. H., Transformation toughening in ZrO_2-containing ceramics. *J. Am. Ceram. Soc.*, 1987, **70**, 689–698.
4. Miller, T. M. and Grassian, V. H., Environmental catalysis: adsorption and decomposition of nitrous oxide on zirconia. *J. Am. Chem. Soc.*, 1995, **117**, 10969–10975.
5. P. Durán, Navarro, L. M., Recio, P. and Jurado, J. R., Processing and properties of zirconia-based/Al_2O_3 nanoscale-composites as electrolytes for solid oxide fuel cells. *Eur. J. Solid State Inorg. Chem.*, 1995, **32**, 963–975.
6. Moya, J. S., Sánchez-Herencia, A. J., Moreno, R., Pena, P. and Requena, J. Layered ceramic composites: a new family of advanced materials. In *Third Euro-Ceramics*, Vol. 3, ed. P. Durán and J. F. Fernández. Faenza Eritrice Ibérica S. L., Spain, 1993, pp. 289–300.
7. Garvie, R. C., The ocurrence of metastable tetragonal zirconia as a crystallite size effect. *J. Physical Chemistry*, 1965, **69**, 1238–1243.
8. Lange, F. F., Transformation toughening, part 3: experimental observations in the ZrO_2–Y_2O_3 system. *J. Mater. Sci.*, 1982, **17**, 240–246.
9. Heuer, A. H., Claussen, N., Kriven, W. M. and Rühle, M., Stability of tetragonal ZrO_2 particles in ceramic matrices. *J. Am. Chem. Soc.*, 1982, **65**, 642–650.
10. Garvie, R. C. and Goss, M. F., Intrinsic size dependence of the phase transformation temperature in zirconia microcrystals. *J. Mater. Sci.*, 1986, **21**, 1253–1257.
11. Mercera, P. D. L., van Ommen, J. G., Doesburg, E. B. M., Burggraaf, A. J. and Ross, J. R. H., Stabilized tetragonal zirconium oxide as a support for catalysts: evolution of the texture and structure on calcination in static air. *Appl. Catal.*, 1991, **78**, 79–96.
12. Huang, D., Venkatachari, K. R. and Stangle, G. C., Influence of the yttria content on the preparation of nanocrystalline yttria-doped zirconia. *J. Mater. Res.*, 1995, **10**, 762–773.
13. Turlier, P., Dalmon, J. A., Martin, G. A. and Vergnon, P., Non-porous stabilized ZrO_2 particles as support for catalysts. *Appl. Catal.*, 1987, **29**, 305–310.
14. Alvarez, M. R. and Torralvo, M. J., Textural characterisation of zirconia and yttria-doped zirconia powders. *Colloids and Surface A*, 1994, **83**, 175–182.

15. Álvarez, M. R. and Torralvo, M. J., Textural evolution of zirconia and yttria-doped zirconia on thermal treatment under different conditions. *Colloids and Surface A*, 1996, **113**, 165–174.
16. Payne, D. A., Sing, K. S. W. and Turk, D. H., Comparison of argon and nitrogen adsorption isotherms on porous and nonporous hydroxilated silica. *J. Colloid Interf. Sci.*, 1973, **43**, 287–293.
17. Pierce, C., Computation of pore sizes from physical adsorption data. *J. Phys. Chem.*, 1953, **57**, 149–152.
18. McClellan, A. L. and Harnsberger, H. F., Cross-sectional areas of molecules absorbed on solid surfaces. *J. Colloid Interf. Sci.*, 1967, **23**, 577–599.
19. Broekhoff, J. C. P. and De Boer, J. H., Studies on pore systems in catalysts, Part XI: pore distributions calculations from the adsorption branch of a nitrogen adsorption isotherm in the case of "ink-bottle" type pores. *J. Catal.*, 1968, **10**, 153–165.
20. Yoshimura, M., Phase stability of zirconia. *Ceramic Bulletin*, 1988, **67**, 1950–1955.
21. Rijnten, H. Th., Formation, preparation and properties of hydrous zirconia. In *Physical and Chemical Aspects of Adsorbents and Catalysts*, ed. B. G. Linsen. Academic Press, London, 1970, pp. 315–371.
22. Crucean, E. and Rand, B., Calcination of zirconia gels. *Trans. J. Brit. Ceram. Soc.*, 1979, **78**, 58–64.
23. Gimblett, F. G. R., Rahman, A. A. and Sing, K. S. W., The origin of porosity in hydrous zirconia gel: I. Microporous gels. *J. Colloid Interf. Sci.*, 1981, **84**, 337–345.
24. Mercera, P. D. L., van Ommen, J. G., Doesburg, E. B. M., Burggraaf, A. J. and Ross, J. R. H., Zirconia as support for catalysts: evolution of the texture and structure on calcination in air. *Appl. Catal.*, 1990, **57**, 127–148.
25. Turrillas, X., Barnes, P., Gascoigne, D., Turner, J. C., Jones, S. L., Norman, C. J., Pygall, C. F. and Dent, A. J., Synchroton-related studies on the dynamic and structural aspects of zirconia synthesis for ceramic and catalytic applications. *Radiat. Phys. Chem.*, 1995, **45**, 491–508.
26. Clearfield, A., The mechanism of hydrolitic polymerization of zirconyl solutions. *J. Mater. Res.*, 1990, **5**, 161–162.
27. Haberko, K., Characteristics and sintering behaviour of zirconia ultrafine powders. *Ceramurgia International*, 1979, **5**, 148–154.
28. Schultz, M., Grimm, St. and Burckhardt, W. The isoelectric point of pure and doped zirconia in relation to the preparation route. *Solid State Ionics*, 1993, 63–65, 18–24.
29. Parks, G. A., The isoelectric points of solid oxides, solid hydroxides and aqueous hydroxo complex systems. *Chem. Rev.*, 1965, **65**, 177–198.
30. Kagawa, M., Omori, M., Syono, Y., Imamura, Y. and Usui, S., Surface characterization of zirconia after reaction with water. *J. Am. Ceram. Soc.*, 1987, **70**, C212.
31. Lange, F. F., Transformation toughening, Part 1: size effects associated with the thermodynamics of constrained transformations. *J. Mater. Sci.*, 1982, **17**, 225–234.